

In Situ Combustion of Heavy, Medium, and Light Crude Oils: Low-Temperature Oxidation in Terms of a Chain Reaction Approach

Alexandra S. Ushakova, Vladislav Zatsepin, Mohammed A. Khelkhal,* Sergey A. Sitnov, and Alexey V. Vakhin*



Cite This: *Energy Fuels* 2022, 36, 7710–7721



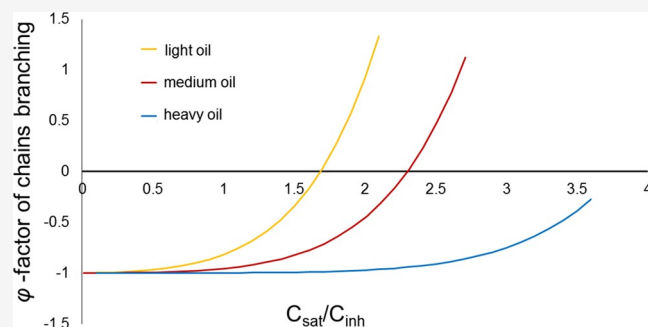
Read Online

ACCESS |

Metrics & More

Article Recommendations

ABSTRACT: Oil oxidation reactions have attracted considerable interest in terms of mechanism comprehension for thermally enhanced oil recovery applications. Many hypotheses regarding oil oxidation mechanisms appear to be disputable even now. The aim of our work was to broaden current knowledge on the crude oil oxidation chain reaction mechanism including the formation behavior of free radicals and hydroperoxides. In this context, we attempted to shed light on the main differences in the oxidation reactions between heavy and light oils. We have found a way to solve both analytically and numerically a set of differential equations for concentrations corresponding to the reaction scheme. Taken together, our findings allowed us to obtain hydroperoxide concentration dependence on time for the initial stages of oxidation. Two main time dependencies were observed, one for low-temperature oxidation (LTO) and the other for high-temperature oxidation (HTO). Both dependencies were revealed in the oxidation experiments of different types of oils and were taken for the matching procedure, which is also presented in this work. The φ -factor of branched-chain reactions, obtained as a combination of reaction rates, determines the efficiency of LTO and transition from LTO to HTO. By matching the experimental data, we were able to find that the success of self-ignition may be achieved only if the concentration ratio of saturated hydrocarbons to inhibitors in crude oil is equal to 2 or more and the temperature is more than 415 K. Under these conditions, the ignition time for heavy oil was 5–7 days, and that for light oil was 15–30 min in oxidation experiments, which were well matched by the presented chain reaction model.



1. INTRODUCTION

For many years, there has been a rapid increase in the successful implementation of air injection into reservoirs for enhancing oil recovery around the world.^{1–3} For the past 40 years, in situ combustion (ISC) has been implemented for enhancing heavy oil recovery; meanwhile, high-pressure air injection (HPAI) has been implemented for light oil extraction. In fact, the main reason for injecting air into an oil reservoir is to form a combustion front, which results in heat generation and, therefore, effective oil displacement.^{4–8} However, the formation and stabilization of the combustion front are widely based on the oxidation reaction rate, which mainly depends on reservoir conditions and its oil properties. In other words, the more stable the combustion front is, the safer and more efficient the implementation of air injection turns out to be.⁹ It is common knowledge that the air injection effect differs from one oilfield to another, and it significantly depends on the tendency of oil to oxidation. In the classical approach, crude oil oxidation can be divided into two main types of reactions: low-temperature oxidation and high-temperature oxidation reactions (LTO and HTO, respec-

tively).^{6,8,9} Moreover, the intensity of oxidation and the transition from LTO to HTO is a significant question for each air injection pilot, which is also related to in situ oil self-ignition or artificial ignition.^{8,10,11}

Various approaches have been proposed to obtain reliable models for the ignition process of oxidation, which resulted in a wide range of literature and experimental studies on the initial stages of crude oil oxidation, mutual influence of oil components on the process, and also theoretical approaches to this item.^{12–27}

The experimental studies on the initial stages of crude oil oxidation were oriented toward exploring the possibility of self-ignition. There are two main oxidation experiments, namely, adiabatic and isothermal experiments, performed to explore

Received: March 31, 2022

Revised: June 14, 2022

Published: June 28, 2022



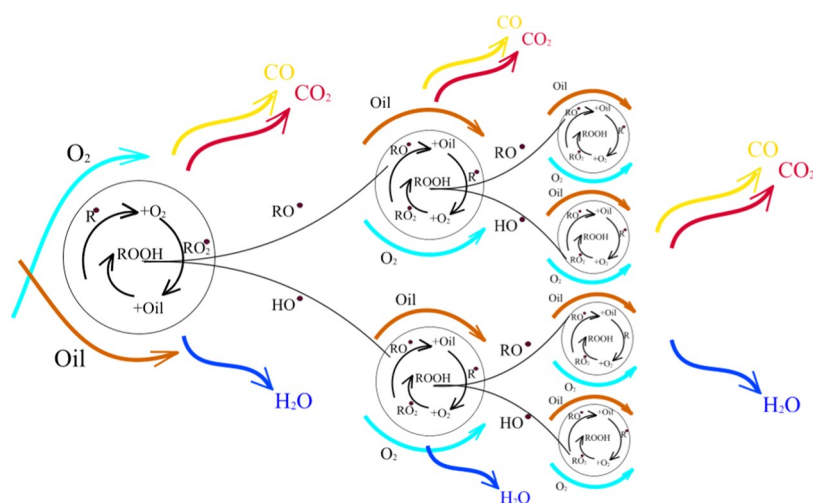


Figure 1. Chain reaction mechanism of crude oil oxidation.

initial oxidation stages. Actually, isothermal conditions allow us to obtain kinetic parameters in accordance with the parameters of outgoing gases and variation in oil properties with time.^{22–25,28} This means that temperatures are usually low for combustion, and oxygen addition reactions are observed. In the adiabatic experiments (adiabatic tube or accelerating rate calorimeter (ARC)), the temperature increases gradually until the exothermal effect of the reaction and self-heating effect starts; after that, the equipment follows the initial reaction heat release to explore the reaction without an external influence.^{23,29} These experiments can be performed at the reservoir temperature and higher temperatures as well. In fact, adiabatic experiments may ease exploring the quick process of oxidation, which leads to HTO reactions. It is worthwhile noting that both isothermal and adiabatic oxidation experiments describe the initial stages of oxidation. However, isothermal oxidation usually performs LTO reactions, and adiabatic oxidation performs HTO reactions. In addition, HTO reactions are also performed with a pressurized differential scanning calorimeter (PDSC), which is also widely used for crude oil oxidation studies.^{27,30–34}

The recent articles in the area of in situ combustion show a tendency to a less-complicated description of in situ combustion reactions but a more comprehensive approach, including all of the stages of experimental data, their interpretation, adaptation, and representation into modeling parameters, and computer simulation of the combustion process in addition to oil recovery prediction.^{8,34} Even the group of investigators who previously developed very complicated in situ combustion models and successfully described processes such as evaporation, cracking, and changes in fuel deposits^{8,11,21} also considered the three components to be more convenient for further modeling procedures.³⁵ We also follow this tendency to adapt the experimental results for further simulation processes.

Some preliminary work was carried out on both types of experiments, high-rate adiabatic experiments and low-rate isothermal experiments, in terms of the chain reaction mechanism of the initial stages of oxidation.¹⁶ The chain reaction approach suggested for the crude oil oxidation in ref 17 and then developed in ref 19 as the term of chemical reactions has shown a good agreement with experimental results. In addition, the phenomenological description of the

chain reaction mechanism of oxidation helped to deduce dependencies obtained in both types of experiments.¹⁶ The first few systematic studies have attempted to obtain general mechanisms for all oxidizing oils independently on the experimental equipment type and found significant differences between light and heavy oil oxidation in both processes as well.¹⁶

The next challenge was to achieve a strictly theoretical approach for the initial stages of both processes, low-rate and high-rate oxidation. With regard to the aim of the present work, we started a mathematical description of the chain reaction approach for the initial stages of oxidation to describe the experimental results, express the differences between heavy and light oil samples in mathematical form, and conduct some primary work for the novel simulation opportunities.

2. METHODOLOGY

2.1. Chain Reactions Theory. As mentioned in a great number of papers based on different experiments using different techniques, the crude oil oxidation process usually includes the following stages:^{6,11,20,35}

1. Oxygen consumption.
2. Release of CO and CO₂ gases.
3. Appearance of oxidized components.
4. Heat release due to oxidation
5. Reaction acceleration or decay.

The first investigation on oil oxidation mechanisms found that reaction models are usually written down for some oil component oxidation or pseudocomponents. However, such simplification could be suitable for modeling but could not refer to the whole complex picture of the oxidation process.^{12,13,20,23,28} On the other hand, including too many components complicates the process of isolating the most important ones.³⁵

According to the literature, the rate-limiting step of the oxidation process is the accumulation of hydroperoxides.^{36–38} First, oxygen molecules penetrate into the oil chains and form free radicals. Then, the radicals pass from one molecule to another (chain growth) until they form hydroperoxides. In addition, some products of the reactions lead to the formation of CO, CO₂, water, oxidized components, aldehydes, ketones, and acids. This stage has been widely investigated, and it is commonly known as low-temperature oxidation. Additionally,

the hydroperoxides can decompose into a pair of radicals: this is a branching chain reaction.^{39,40} In fact, the new radicals initiate the new chains and start new oxidation processes (Figure 1). This process self-accelerates and causes the ignition of oil. It is usually observed in accelerating rate calorimeter experiments of oil ignition.³⁷ It has been found that an increase in the temperature causes nonradical high-temperature oxidation where the chain reaction mechanism takes place, although it has been reported that it is not the main one. Broadly speaking, at high temperatures, above 523.15 K, hydroperoxides decompose without the radical mechanism.⁴¹

However, this is not particularly surprising if we consider active and inactive oil components at the initial oxidation stages. Both of these compounds oxidize simultaneously, but they lead to different products. This approach involves simplification because the active oil components at the initial stages can become inactive. This has been mentioned in ref 17, which reported that crude oil separates into the following main oxidizing components, alkanes (denoted as sat) and their oxidation inhibitors in addition to aromatic compounds, which then form the fuel (denoted as In *h*).

Until now, the oxidation of saturated hydrocarbons has been considered as the most studied process.^{17,42,43} In their recent work, Yuan and Freitag et al. have carried out experiments on the oxidation of crude oil, oil saturates, and synthetic hydrocarbons using high-pressure differential scanning calorimetry (HPDSC).^{14,17} It has been reported that hydroperoxides are the only primary oxidation products for saturated hydrocarbons, which is in agreement with the results obtained in ref 24. Moreover, it has been found that the crude oil contained about 70–75% of saturated hydrocarbons, 20% of aromatic compounds, and about 5–10% of resins and asphaltenes.

2.2. Chemical Reactions of Low-Temperature Oxidation. The initial studies of hydrocarbon oxidation show that oxidation always proceeds by breaking the C–H bond, both in the branched-chain and unbranched processes.^{39,41} Liquid hydrocarbons are resistant to dissociation of the C–C bond up to 473.15 K. So, the initial set of reactions is expressed as follows



where R^\bullet is the alkyl radical, and the initiation rate at this stage depends on the concentrations according to $v_0 = k_1 C_{\text{sat}} C_{\text{O}_2}$.

In the following step, free radicals again enter into the chain propagation reactions, which can be written as in ref 17



where RO_2^\bullet is an alkyl peroxy radical. In fact, the chain growth herein depends on the radical formation rate. Then, the radical reaction produces hydroperoxides, which are the major oxidation products at the primary oxidation stages.

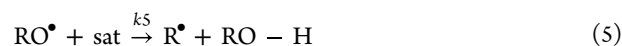


where ROOH is the hydroperoxide. At this stage, hydroperoxide radicals react almost instantly, as their activation energy is very small. According to ref 26, the bond strength of O–O is about 160–200 kJ/mol, which is smaller than the bond strengths of O–H (~480 kJ/mol) and O–C (~380 kJ/mol). For this reason, hydroperoxides are the most unstable among the obtained oxidized oil compounds.

The hydrocarbon hydroperoxides are decomposed by a monomolecular mechanism on two free radicals as in reaction 4



At this moment, hydroperoxides may accumulate in the system, especially if the temperature is low (100–200 °C). According to electron paramagnetic resonance (EPR) spectroscopy experiments, the concentration of organic radicals obtained by hydroperoxide decomposition increases twice with the temperature increasing up to 170 °C.⁴⁴ For higher temperatures, the number of free radicals reaches dynamic equilibrium. RO^\bullet and OH^\bullet radicals further interact with oil and continue to form new chains through the reaction

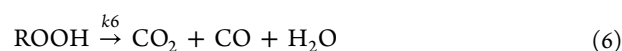


In fact, the radical RO^\bullet results in the formation of a new radical R^\bullet , thus serving as an autocatalyst in the system.

The above reactions all refer to the LTO process, where the initial set of equations for oxidation initiation, free radical appearance, and hydroperoxide formation is present.

Reactions 1–5 govern the process of the LTO stage, describe the appearance of oxidized components (3), and decomposition (4 and 5) reactions. From such a point of view, it is not necessary to distinguish bond scission reactions and oxygen addition reactions as in ref 11 as independent processes.

The schematic illustration of the LTO oxidation stages is shown in Figure 1. It shows the cyclic character of the oxidation through radical appearance and hydroperoxide accumulation. The more the hydroperoxides are accumulated, the higher is the oxidation rate. Moreover, the decomposition of hydroperoxides significantly accelerates the oxidation as it leads to the branching of chains—the formation of two radicals at a time according to reaction 4. In addition to chain branching, hydroperoxides can undergo transformations at temperatures higher than 200 °C by the nonradical mechanism with complete combustion to CO, CO₂, and water.



The decomposition of hydroperoxides is an oxidation stage where the dependence of the reaction rate on the oxygen concentration is reduced. This led authors in ref 17 to report that this confines to the negative temperature gradient.

In addition to the aforementioned set of eqs 1–6, other ways of free radical escape could be considered as well. In other words, a quadratic break of radicals with the formation of alcohols and ketones can occur by the reactions $\text{R}^\bullet + \text{R}^\bullet \rightarrow \text{R}-\text{R}$, $\text{RO}_2^\bullet + \text{R}^\bullet \rightarrow \text{RO} - \text{OR}$, or the most probable reaction $\text{RO}_2^\bullet + \text{RO}_2^\bullet \rightarrow \text{RO} - \text{OR} + \text{O}_2$.

The deceleration and acceleration of radical reactions, caused by small additions of catalysts or inhibitors, are possible at the stage of radical oxidation. In fact, crude oil can initially contain these compounds, or they can be formed during the initial stages of oxidation. Most likely, the features of light and heavy oil oxidation are associated with the presence of substances that affect the oxidation process at the stage of chain growth by a radical mechanism.²⁴

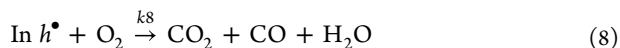
Generally speaking, we consider the following main inhibition reaction:



Reaction 7 is an oxygenation reaction without further development of combustion, which leads to a high molecular residue. This process causes fuel formation at low temperatures; in fact, this process together with **reaction 5** leads to the formation of inactive hydroperoxides or well-known oxygen addition reactions.

According to the current terminology, all substances that burn with heat release in the temperature range of 723–873 K are called “fuel for combustion”.^{6,11,12,20,21} Fuel, often also called “Coke” in the literature, is generated during the oxidation process from aromatic, cyclic, and even saturated hydrocarbons.^{11,13,20,21}

The complete combustion reaction is the continuation of **reaction 7**, which ends the system of chemical reactions:



It is generally accepted that **reactions 1–8** express the simplest example of the chain reaction process without any detailed consideration of the oil structure. This can be indeed applied to heavy and light oils as well. The first few studies on oil oxidation suggest that reaction rates obey the Arrhenius law as expressed by the equation

$$k_i = A_{0i} \cdot \exp\left(-\frac{E_i}{RT}\right) \quad (9)$$

In this paper, k_1 represents the initiation rate and chain transfer rates are represented as k_2 , k_3 , and k_5 , chain branching rate as k_4 , chain termination rate as k_7 , nonradical complete combustion of hydroperoxide rate as k_6 , and the residue combustion rate as k_8 . It is worthwhile noting that all of the reaction rates will be considered dimensionless for further calculation.

Here and further manipulating with these equations, we keep in mind that the most significant initial stages of oxidation are the reactions of hydroperoxide formation (3) and hydroperoxide recombination (4 and 7). As shown in **Figure 1**, these stages supply the chain growth and chain branching, which are considered the main significant keys in the initial stages of combustion. These are the main differences that distinguish the present approach from similar studies where chain reactions are often omitted from consideration because of their low heat output.

2.3. System of Differential Equations. Our next procedure will be fulfilled by solving the system of equations to obtain the dependence of hydroperoxide concentration on time, so as to describe the main dependencies of light and heavy oil oxidation processes from initiation, through the LTO stage, until complete combustion.

Despite the simple reaction scheme provided in the present work, solving differential equations based on concentrations, however, is very complicated and requires some simplification unable to influence the description of the main processes. Therefore, the following approximations have been taken into consideration to simplify the system of equations:

- (1) First, the activity of any alkoxy radical RO^{\bullet} is considered equal to the activity of the hydroxyl $\bullet\text{OH}$ radical, which suggests that these particles are indistinguishable. This leads to transforming **reaction 4** into $\text{ROOH} \xrightarrow{k_4} 2\text{RO}^{\bullet}$
- (2) Next, HO_2^{\bullet} radicals are considered to be less active, and thereby they are not included in the reaction scheme.

- (3) Then, the quadratic break of free radicals is considered to occur rarely compared to chain termination by inhibitors (7).
- (4) On the other hand, we considered the reaction rate of initiation reaction as being constant during hydroperoxide formation ($\nu_0 = k_0 C_{\text{O}_2} C_{\text{sat}} = \text{const}$). This is approved because we consider the dependence of hydroperoxide concentration on time at rather low temperatures—concentration from reservoir temperature till 403–413 K.
- (5) Finally, in our study, only LTO stages and the chain reaction mechanism are taken into consideration without taking into consideration the complete combustion **reactions 6** and **8**. In other words, our study focuses only on the radical mechanism and the dependence of hydroperoxide concentration on time, in addition to the dependence on other parameters on time variation.

It is important to note that unlike previous work,¹⁹ we considered a much simplified scheme of low-temperature oxidation and did not include high-temperature oxidation reactions. Nevertheless, we have provided a complete analysis of the obtained results in terms of simplifications and focused on the differences between light and heavy oil oxidation to connect the phenomenological approach described in ref 16 with the chemical reaction scheme.

For LTO stages, we simply considered the system of differential equations for the **reaction schemes 1–5** with **7** for the destruction of radicals

$$\frac{\partial}{\partial t}(C_{\text{O}_2}) = -k_1 C_{\text{sat}} C_{\text{O}_2} - k_2 C_{\text{R}^{\bullet}} C_{\text{O}_2} \quad (10)$$

$$\frac{\partial}{\partial t}(C_{\text{sat}}) = -k_1 C_{\text{sat}} C_{\text{O}_2} - k_3 C_{\text{sat}} C_{\text{RO}_2^{\bullet}} - k_5 C_{\text{sat}} C_{\text{RO}^{\bullet}} \quad (11)$$

$$\frac{\partial}{\partial t}(C_{\text{P}}) = k_3 C_{\text{sat}} C_{\text{RO}_2^{\bullet}} - k_4 C_{\text{P}} \quad (12)$$

And for the radicals

$$\begin{aligned} \frac{\partial}{\partial t}(C_{\text{R}^{\bullet}}) &= k_1 C_{\text{sat}} C_{\text{O}_2} + k_3 C_{\text{sat}} C_{\text{RO}_2^{\bullet}} - k_2 C_{\text{R}^{\bullet}} C_{\text{O}_2} \\ &\quad + k_5 C_{\text{sat}} C_{\text{RO}^{\bullet}} \end{aligned} \quad (13)$$

$$\frac{\partial}{\partial t}(C_{\text{RO}^{\bullet}}) = k_4 C_{\text{P}} - k_5 C_{\text{sat}} C_{\text{RO}^{\bullet}} \quad (14)$$

$$\frac{\partial}{\partial t}(C_{\text{RO}_2^{\bullet}}) = k_2 C_{\text{R}^{\bullet}} C_{\text{O}_2} - k_3 C_{\text{sat}} C_{\text{RO}_2^{\bullet}} - k_7 C_{\text{In } h} C_{\text{RO}_2^{\bullet}} \quad (15)$$

For a more convenient view, we have used P as an index for hydroperoxide instead of ROOH.

Bodenstein's principle of quasistationary concentration can be applied to the equations with radicals **13–15** because the reaction rate of radical formation is much lower than the rate of radical's decay. These equations can be converted into algebraic form and solved relative to the concentration of peroxides, saturates, and oxygen

$$\frac{\partial}{\partial t}(C_{\text{RO}_2^{\bullet}}) = \frac{\partial}{\partial t}(C_{\text{R}^{\bullet}}) = \frac{\partial}{\partial t}(C_{\text{RO}^{\bullet}}) = 0$$

To solve eqs 10–12 in an explicit form, it is necessary to express the concentration of radicals via the concentration of peroxides.

$$C_{RO\cdot} = C_P \frac{k_4}{k_5 C_{sat}} \quad (16)$$

$$C_{RO_2\cdot} = \frac{(k_1 C_{sat} C_{O_2} + k_4 C_P)}{k_7 C_{Inh}} \quad (17)$$

$$C_R\cdot = (k_3 C_{sat} / k_7 C_{Inh} + 1) \frac{(k_1 C_{sat} C_{O_2} + k_4 C_P)}{k_2 C_{O_2}} \quad (18)$$

The differential equations for peroxides, oil, and oxygen concentrations can be written as

$$\left\{ \begin{aligned} \frac{\partial}{\partial t}(C_{O_2}) &= (k_3 C_{sat} / k_7 C_{Inh} + 1)(k_1 C_{sat} C_{O_2} + k_4 C_P) \\ &\quad - k_1 C_{sat} C_{O_2} \end{aligned} \right. \quad (19)$$

$$\left\{ \begin{aligned} \frac{\partial}{\partial t}(C_P) &= k_1 C_{sat} C_{O_2} + (k_3 C_{sat} / k_7 C_{Inh} - 1) \\ &\quad (k_1 C_{sat} C_{O_2} + k_4 C_P) \end{aligned} \right. \quad (20)$$

$$\left\{ \begin{aligned} \frac{\partial}{\partial t}(C_{sat}) &= -(k_3 C_{sat} / k_7 C_{Inh} + 1)(k_1 C_{sat} C_{O_2} \\ &\quad + k_4 C_P) \end{aligned} \right. \quad (21)$$

In fact, this system can be solved numerically, but as we want to obtain the dependence of the main parameters in an implicit way, we introduced some simplifications as follows:

- (1) The constant reaction rate of initiation discussed before simplifying the system does not allow the consideration of the rapid change in oxygen and saturates ($v_0 = k_0 C_{O_2} C_{sat} = \text{const}$).
- (2) We assume that at the initial stages of oxidation concentrations, C_{sat} and C_{O_2} do not change significantly.

Let us consider the following series: $C_{O_2} = C_{O_2}^0 + \Delta C_{O_2}$, $\Delta C_{O_2} \ll C_{O_2}^0$ and $C_{sat} = C_{sat}^0 + \Delta C_{sat}$, $\Delta C_{sat} \ll C_{sat}^0$

As a result, the set of the equations could be rewritten as

$$\left\{ \begin{aligned} \frac{\partial}{\partial t}(C_P) &= \left(\frac{k_3 C_{sat}^0}{k_7 C_{Inh}} - 1 \right) k_4 C_P + v_0 \frac{k_3 C_{sat}^0}{k_7 C_{Inh}} \end{aligned} \right. \quad (22)$$

$$\left\{ \begin{aligned} \frac{\partial}{\partial t}(\Delta C_{sat}) &= - \left(\frac{k_3 (C_{sat}^0 + \Delta C_{sat})}{k_7 C_{Inh}} + 1 \right) \\ &\quad (k_4 C_P + v_0) \end{aligned} \right. \quad (23)$$

The equation for oxygen concentration is not included in the system; it can be solved separately after the system (22 and 23). So, the differential equation for the concentration of hydroperoxides can be solved separately, and eq 22 can be integrated. Let us denote the factor of degenerate branching φ as $\varphi = k_4^* ((k_3 C_{sat}) / (k_7 C_{Inh}) - 1)$, according to Semenov's theory.^{37,41}

$$\frac{\partial}{\partial t}(C_P) = \varphi C_P + \frac{k_3 C_{sat}^0}{k_7 C_{Inh}} v_0 \quad (24)$$

As we have fixed the initiation reaction rate, we have to also fix a certain induction period of time τ until which the hydroperoxide concentration has zero value, $\tau \sim 1/v_0$ and $C_P(\tau) = 0$. The resulting dependence for hydroperoxide concentration has exponential time dependence as described in (25)

$$\varphi C_P = \frac{k_3 C_{sat}^0}{k_7 C_{Inh}} v_0 [e^{\varphi(t-\tau)} - 1] \quad (25)$$

For the concentration shift of saturates ΔC_{sat} , one can obtain an approximate formula by integrating (22) taking into account (25)

$$\Delta C_{sat} = - \frac{k_3 C_{sat}^0 + k_7 C_{Inh}}{k_7 C_{Inh}} \left(k_4 \frac{k_3 C_{sat}^0}{k_7 C_{Inh}} \frac{v_0}{\varphi^2} [e^{\varphi(t-\tau)} - 1 - \varphi(t-\tau)] + v_0(t-\tau) \right) \quad (26)$$

And the corresponding dependence of oxygen concentration shift on time ΔC_{O_2} would be written as

$$\Delta C_{O_2} = - \frac{k_3 C_{sat}^0 + k_7 C_{Inh}}{k_7 C_{Inh}} v_0 (t-\tau) - k_4 v_0 \left(\frac{k_3 C_{sat}^0}{k_7 C_{Inh} \varphi} \right)^2 [e^{\varphi(t-\tau)} - 1 - \varphi(t-\tau)] \quad (27)$$

The results 26 and 27 can be simplified because we considered the expansion in the small parameters ΔC_{sat} and ΔC_{O_2} for a short period of time and low φ values

$$\Delta C_{sat} = - \frac{k_3 C_{sat}^0 + k_7 C_{Inh}}{k_7 C_{Inh}} \left(v_0(t-\tau) + k_4 v_0 \frac{k_3 C_{sat}^0}{k_7 C_{Inh}} \frac{(t-\tau)^2}{2} \right) \quad (28)$$

$$\Delta C_{O_2} = - \frac{k_3 C_{sat}^0 + k_7 C_{Inh}}{k_7 C_{Inh}} v_0 (t-\tau) - k_4 v_0 \left(\frac{k_3 C_{sat}^0}{k_7 C_{Inh}} \right)^2 \frac{(t-\tau)^2}{2} \quad (29)$$

So, both dependencies obtained for oxygen and oil in low-temperature oxidation decrease linearly with time. This is a result of a very rough approximation, but it was done to drive out analytical formula 25 for the dependence of hydroperoxide concentration on time. This dependence agrees with the usual phenomenological dependencies for hydrocarbon oxidation considered in ref 16 and observed in many experimental studies.

3. RESULTS AND DISCUSSION

3.1. Modeling. The aforementioned calculations helped us to eliminate the dependence of hydroperoxide concentration on time. Specifically, in our study on the chain reaction oxidation mechanism, all of the products are formed through the stage of hydroperoxides. So, all of the transitions in the oxidation system are connected with hydroperoxide appearance and decay. This is reflected in reactions 1–5.

First, let us consider the obtained exponential dependence of hydroperoxides on time (25). The φ -factor of degenerate branching was obtained as a combination of reaction rates of

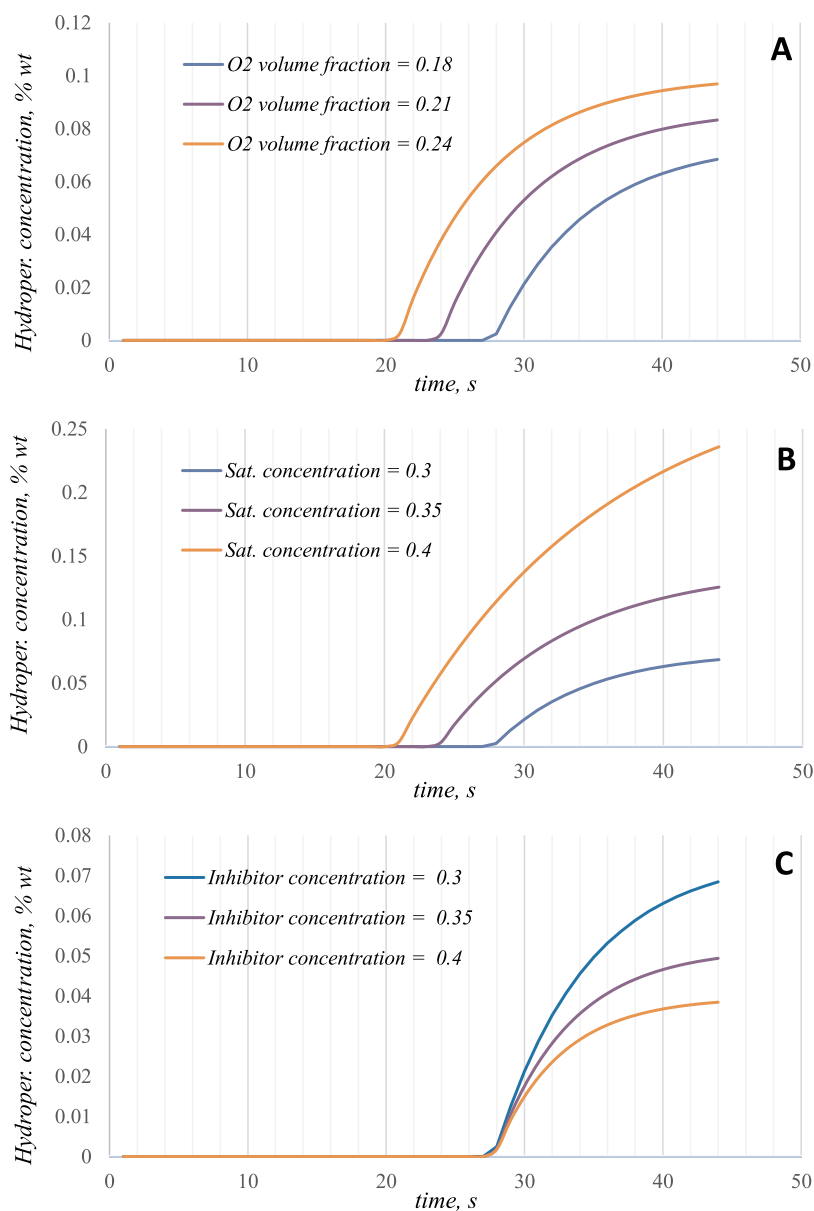


Figure 2. Calculation of the dependence of hydroperoxide concentration on time for the negative j -factor (A, with different initial volume fraction of oxygen; B, different initial saturate concentrations; C, different inhibitor concentrations).

free radical appearance (reaction 3), and their capture by inhibitors (reaction 7) in experimental works was very small, about $\pm 0.1\text{--}0.01\text{ s}^{-1}$. The value of the φ -factor is also proportional to the reaction rate of hydroperoxide appearance (reaction 4); the concentrations of active saturates as the source of free radicals, and the concentration of inhibitors are both present in the formula for φ .

The negative φ -factor is caused by the inhibition process (reaction 7) dominating the free radical appearance (reaction 3). In this case, hydroperoxide formation with time has limited growth from zero value until the limiting value:

$$C_p = \frac{k_3 C_{\text{sat}} v_0}{k_7 C_{\text{in } h} |\varphi|} [1 - e^{-|\varphi|(t-\tau)}], C_p \rightarrow v_0 / \varphi (k_3 C_{\text{sat}}) / (k_7 C_{\text{in } h}) \quad (30)$$

As a result, this process causes limited temperature growth, small heat output, and the absence of high-temperature

oxidation. In this case, the formation of the oxidized component could be observed by the exponential law $\sim 1 - \exp(-|\varphi|t)$, common for the LTO process. The formula (25) with $\varphi > 0$ reflects the case of the high-rate oxidation process with exponential growth of hydroperoxide concentration. The calculated time dependencies for hydroperoxide concentrations in the case of negative and positive φ -factors are presented in Figures 2 and 3, respectively. All of the reaction rates and the concentration of initial components affect the results. First, we consider the constant reaction rates (assume the consideration of hydroperoxide formation under a constant temperature) and examine the dependencies of the initial oxygen, saturates, and inhibitor concentrations. Temperature dependence according to (8) will be presented further.

Figure 2 shows the data on the dependence of C_p concentration on time and three curves under various initial volume fractions of oxygen C_{O_2} . The volume fraction of oxygen reflects its amount in air (poor air mixed with nitrogen or

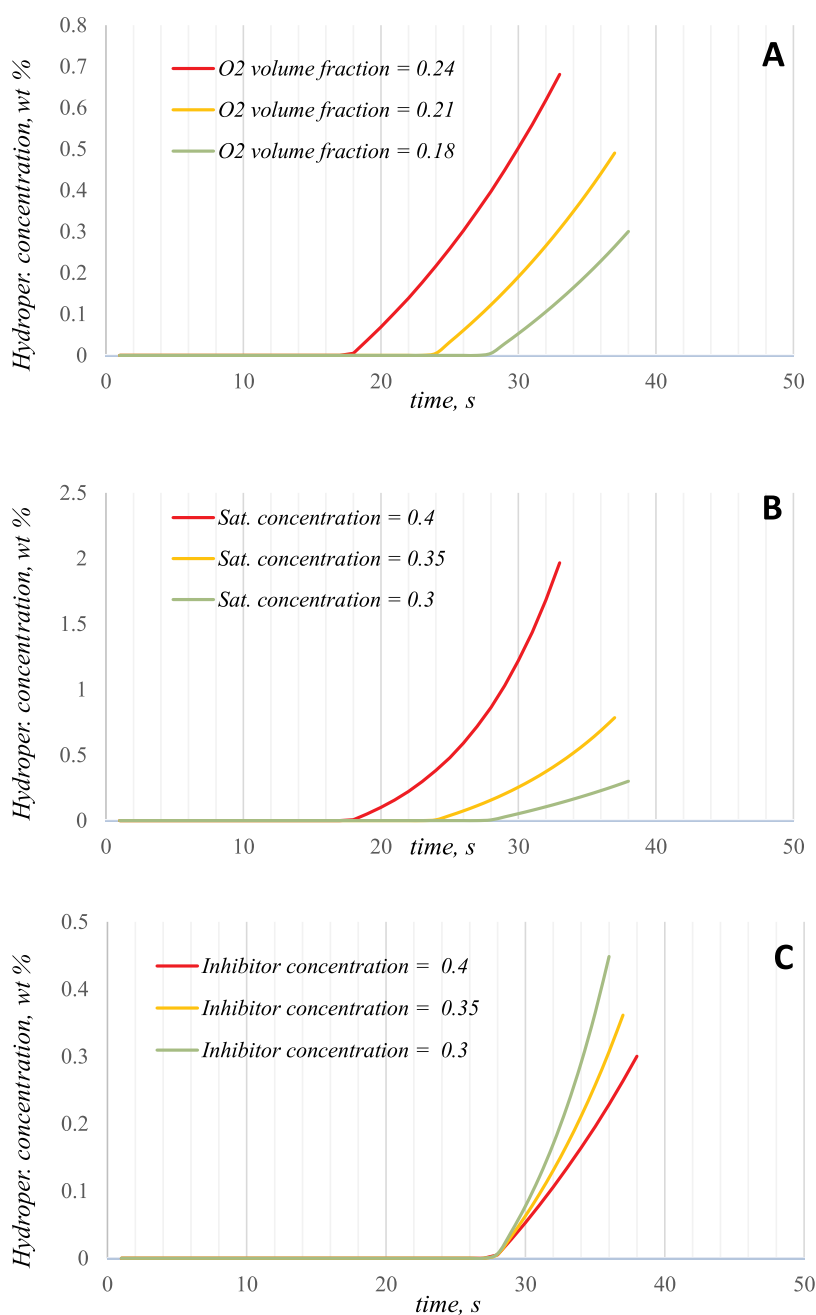


Figure 3. Calculation of the dependence of hydroperoxide concentration on time for the positive φ -factor (A, with different initial volume fractions of oxygen; B, different initial saturate concentrations; C, different inhibitor concentrations).

enriched air) and indeed the pressure and rate of air injection. The questions about the need for enriched air or high rates of air injection for ignition are still of great interest for oilfield pilots. So, here we show the dependence of the hydroperoxide formation on the initial amount of O₂ both for the negative φ -factor (Figure 2a) and the positive φ -factor (Figure 3a). The curve in the middle shows ordinary air where the first one is enriched air; meanwhile, the second one is poor air with oxygen. In both cases (Figures 2a and 3a), the O₂ volume fraction influences the time of the induction period. Broadly speaking, the higher the amount of oxygen is, the earlier the ignition starts, and therefore, the O₂ volume fraction affects the initiation rate. On the other hand, enriched oxygen tends to accelerate the initial oxidation stages. Actually, we do not raise the question of safety here because enriched air can have a high

risk for the safety of ignition procedures. Concerning the poor air with oxygen, it undoubtedly slows down the initiation stage of oxidation. However, as we see with other constant parameters, an increase of the O₂ volume fraction cannot change the negative φ -factor to the positive φ -factor and cannot significantly change the character of oxidation as well.

Next, we consider the influence of initial saturates and inhibitor concentrations on the hydroperoxide amount. According to the selected model, the ratio of saturates to inhibitors indicates the presence of heavy or light oil under oxidation. Heavy components (aromatics, resins) capture the free radicals, and light components (mainly saturates) actively reacting with oxygen. In fact, the effect of saturate concentration on oxidation is the most significant. The positive

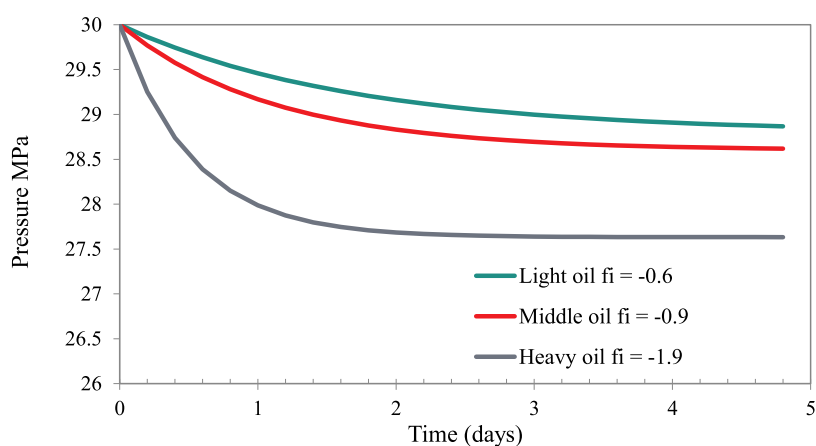


Figure 4. Pressure dropping with time in isothermal oxidation experiments for light, medium, and heavy oils matching procedure.

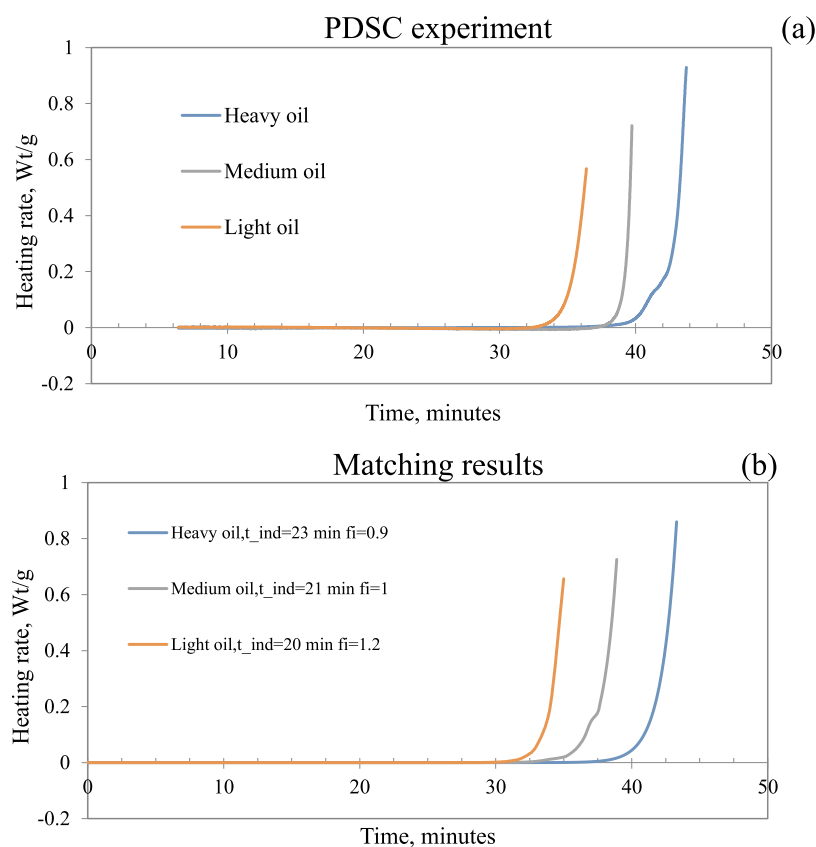


Figure 5. Heat output with time in PDSC experiments for heavy, medium, and light oils in addition to matching procedure results.

φ -factor is plotted in Figure 3b; meanwhile, the negative φ -factor is plotted in Figure 2b.

According to the present model, saturate concentration affects both the time of induction period and the rate of oxidation (hydroperoxide formation), both time and slope of the curves changes (Figures 2B and 3B). The higher the saturate concentration is, the earlier the ignition starts and the faster it proceeds. This is an expected result related to the differences in light and heavy oil technologies. Actually, in situ combustion of heavy oils is mainly based on artificial ignition. However, light oils usually achieve self-ignition based on a high-pressure air injection. As a result, the obtained model reflects these differences for a great acceleration of the oxidation process by increasing the saturate concentration.

It is common knowledge that the inhibitors contained in heavy oil components do not take part in the initial stages, and so they do not affect the value of ignition time. However, these inhibitors can capture a significant volume of free radicals according to the reaction scheme, which affects the oxidation process at later stages. Taken together, the higher the initial concentration of inhibitors is, the lower the increase in the hydroperoxide concentration for both negative and positive φ -factors (Figures 2C and 3C). Therefore, inhibitors are widely believed to slow down the initial oxidation process.

3.2. Data Matching. The above results of hydroperoxide concentration with time have shown rather expected and reasonable dependencies on the initial parameters. In such a way, we have checked the reaction scheme on its coherence

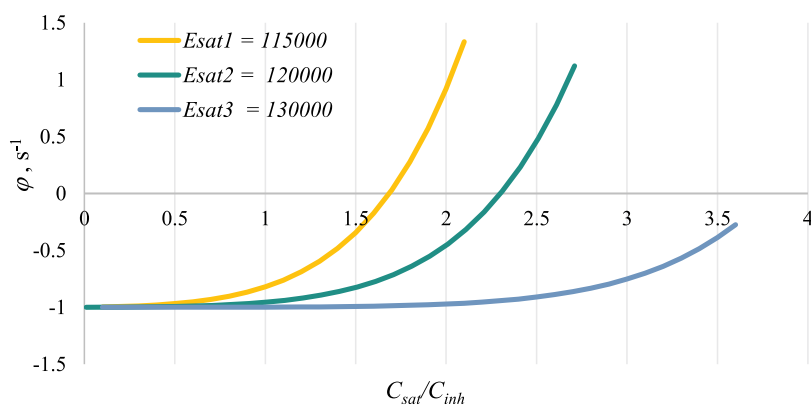


Figure 6. ϕ -factor dependence of $C_{\text{sat}}/C_{\text{inh}}$ varies with temperature at different activation energies of saturate oxidation; inhibitor activation energy is 70 kJ/mol; and reaction rates are similar for C_{inh} and C_{sat} .

with common experimental results. For such reasons, we performed some matching procedure of experimental data with dependencies 25 and 30.

Because of the model's simplicity, the matching procedure was very easy. So, during the experiments, we often observed exponential dependencies of different parameters with time, which are results of hydroperoxide formation at the initial stages of oxidation. Let us consider the low-temperature oxidation experiments held in ref 24. The isothermal oxidation of light, medium, and heavy oil was done in a closed autoclave with a maximum pressure of 30 MPa and a temperature of 393.15 K. The pressure drop with time was evidently observed for the three samples of oil. The process is low-rate oxidation with limited growth of hydroperoxides, which is caused by corresponding oxygen absorption and results in pressure decrease. For the matching procedure, we chose formula 30. The very small negative ϕ factors for $-0.6 \text{ days}^{-1} = -7 \times 10^{-6} \text{ s}^{-1}$ for light oil, $-0.9 \text{ days}^{-1} = -1 \times 10^{-5} \text{ s}^{-1}$ for medium oil, and $-1.9 \text{ days}^{-1} = -2.2 \times 10^{-5} \text{ s}^{-1}$ for heavy oil were defined. The highest value of the negative ϕ -factor for heavy oil was expected because of the highest number of inhibitors (Figure 4). In fact, the small negative ϕ -factor values are mainly related to the slow reaction rate associated with the isothermal mode of oxidation, which has been applied during the repeatability of experiments with the help of the reaction model. In other words, the measurement of system parameters at this stage (pressure variation) proceeded very slowly because the oxidation took place in a closed system at a low temperature (393.15 K). Therefore, we modeled this slow measurement using very small negative ϕ factors. Moreover, small negative ϕ factors are explained by the slow oxidation rates, which result in the slow formation of hydroperoxides as well.

The next challenge was matching the experimental data of pressurized differential scanning calorimetric experiments. The high-rate oxidation in PDSC gives kinetic curves with time. For the matching procedure, we took identical hydrocarbons with different volumes of aromatics. The kinetic experiments and influence of aromatics on oxidation were explored in refs 14, 15. Here, we just focused on initial heat release with time for light, medium, and heavy oils from the PDSC experiments (Figure 5a). The observed exponential growth of heat release with time is caused by the exponential growth of hydroperoxide concentration with the positive ϕ -factor, so formula 25 reflects this case. The matching results are shown in Figure 5b. The induction time decreases from heavy oil (23 min), the lowest amount of saturates, the highest volume of inhibitors

through medium oil (21 min) to light oil (20 min). The light oil shows the highest ϕ -factor ($1.2 \text{ min}^{-1} = 0.02 \text{ s}^{-1}$), with the value for medium oil being $1 \text{ min}^{-1} = 0.017 \text{ s}^{-1}$ and the value for heavy oil being $1.2 \text{ min}^{-1} = 0.015 \text{ s}^{-1}$. The absolute values of the ϕ -factor for high-rate processes are three times higher than that for isothermal oxidation. This is also the expected result and in good consistency with the reaction scheme, where reaction 7 rate k_7 cannot significantly exceed reaction 3 rate k_3 . Otherwise, the chain reaction mechanism will not proceed.

Thus, one can see that the presented reaction scheme did not show any deviations from experimental results and previous views on the mechanism of oxidation and can successfully match experimental data of initial oxidation stages.

4. DISCUSSION

As aforementioned, previous research mostly simplifies the equations of crude oil oxidation, usually by omitting the most part of reactions, which do not support valuable heating rates.^{13,26,37} This approach is reasonable for interpretation and for further modeling but does not fit research on understanding the sources of ignition and the mechanism of transition from LTO to HTO.

The presented reaction model of the initial stages of crude oil oxidation is rather simple. In fact, it is solved for hydroperoxide concentration variation with time in the assumption that all of the other components C_{sat} , C_{O_2} , and C_{inh} are constants. This assumption is approved only for short initial time periods and small temperature variations.

The examples considered above just show the influence of the initial parameters on the process at certain temperatures. Actually, an increase of temperature causes much more significant changes than initial concentrations. All of the reaction rates follow the Arrhenius temperature dependencies expressed by eq 9. Unfortunately, we cannot surely determine all of the Arrhenius parameters. As it was previously discussed in ref 16, only main oxidation stages (with significant gases or heat output) are detected by different experimental techniques, together with kinetic parameter determination. Thus, in this aspect, our model has a rather strict limitation and follows the experimental data only for a rather low temperature (till 400–450 K).

To relaunch the oxidation process with temperature increase, we considered the variation of saturates and inhibitor amount with temperature. The kinetic parameters for modeling were taken from a previous experimental study where light and

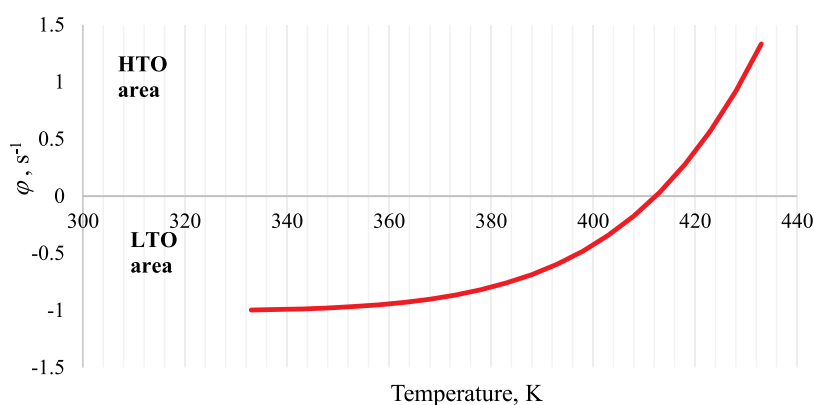


Figure 7. ϕ -factor dependence on temperature for medium oil; $E_{\text{sat}} = 120$ kJ/mol, $E_{\text{in},h} = 70$ kJ/mol.

heavy oil components were characterized in terms of Arrhenius parameters obtained by PDSC.⁴⁵

During the LTO stage, we observed certain waste of active light saturates and following waste of inhibitors as well. According to refs 11, 15, 45, this process is expressed in two peaks of heat release at kinetic curves (usual PDSC kinetic curves of crude oil oxidation). By considering ϕ -factor dependence of ratio $C_{\text{sat}}/C_{\text{In},h}$ Figure 6 shows the increase of the ϕ -factor from negative values to positive in strong dependence on the activation energy of saturate oxidation E_{sat} . As seen, the higher the activity of saturates and the lower the corresponding activation energy, the faster the ϕ -factor increases with temperature.

After the ϕ -factor crosses the zero value, the time dependence (30) changes into exponential growth (25) and low-temperature oxidation turns to high-temperature oxidation (combustion). This point is of great interest for further investigations with more precise models, and it is also connected with the effect of the negative temperature gradient observed in many experiments on crude oil oxidation.^{11,26,27}

The relation $(k_3 C_{\text{sat}})/(k_7 C_{\text{In},h})$ evidently decreases during the oxidation process. But in the case of successful combustion, the active component oxidation heat release increases to a great extent and involves the hydroperoxides in reaction 6 and oxidized components in reaction 8, thus leading to the complete combustion. This case is reflected by the yellow curve (E_{sat} , 115 kJ/mole) and partly by the green curve (E_{sat} , 120 kJ/mole) in Figure 6. Each curve crosses the zero value at a certain $C_{\text{sat}}/C_{\text{In},h}$ ratio. For light oils, this ratio is high enough to reach the HTO region. For heavy oils (blue curve Figure 6), we model the situation when the zero value of the ϕ -factor cannot be reached for reasonable values of the $C_{\text{sat}}/C_{\text{In},h}$ ratio. That means that reactions 1–5 and 7 give insufficient heat release for reaching a positive ϕ -factor value. In other words, heat release is not enough for starting reactions 6 and 8 of complete combustion and the LTO stage ends up with oil degradation and oxidized component formation. So, the unsuccessful process of oxidation is performed in this case.

Figure 7 presents the ϕ -factor increase with temperature. The curve crosses the zero value and indicates the calculated ignition temperature forecasted by the presented reaction scheme (for medium oil, the matched model gives an ignition temperature of 413 K for the experimental conditions of PDSC (pressure 5 MPa, air injection rate of 20 mL/min)). This result shows that the reaction model of chemical equations matched by experimental data are appropriate for the forecasting ignition temperature for air injection pilot projects.

The other significant aspect that concerns the technical issues of air injection implementation is the question of the stable oxidation process and accordingly stable in situ combustion. According to our model, which can describe only the initial stages of oxidation, we can conclude that high values of the $C_{\text{sat}}/C_{\text{In},h}$ ratio (more than 2) and higher temperatures (more than 415 K) lead to exponential self-heating and transition from LTO to HTO. On the other hand, the stability of the combustion front is determined by the amount of fuel burned during HTO, which is also an indirect product of the chain reactions and which is planned to be discussed in future research.

5. CONCLUSIONS

To sum up, the presented reaction scheme has been derived in terms of the chain reaction approach through hydroperoxide formation as the key stage of the oxidation process. The present work has solved the oil oxidation differential equations system in a simple approach, by neglecting oil and oxygen concentration variations during hydroperoxide concentration growth time. Moreover, the resulting dependencies for hydroperoxide concentration with time reflected two main regions of oxidation as being the low-temperature and high-temperature oxidation stages. In addition, the transition from one stage to another stage has been found to be mainly governed by the dependence of hydroperoxide exponential on time by changing the coefficient ϕ -factor of the branched-chain reactions. The novelty of the presented research was in evaluating the ϕ -factor as a combination of reaction rates, which could be negative and positive. Interestingly, its value defined the LTO to HTO transition as well as the ignition temperature. The evidence from the obtained data suggests that the developed model appropriately describes the oxidation process for both light and heavy oils. It has been found that the difference in oil types is basically reflected in the ratio of active saturates to inactive inhibitor concentrations $C_{\text{sat}}/C_{\text{In},h}$. Our investigations in this area have found that both heavy and light oils are able to oxidize in LTO and HTO regions. However, heavy oils have been found to have a longer induction period (5–7 days) because of the stronger inhibition effect compared to light oils, which have been found to have a longer induction period (15–30 min). On the other hand, it has been confirmed that the activation energy values of heavy crude oil samples of the initial oxidation stages are higher than those of light oil samples (130 kJ/mol for heavy oil and 115 kJ/mol for light oil). In this research, we have succeeded in obtaining a reliable model that correlates fairly well with experimental data after

the matching procedure. The prospect of being able to model the process of oil oxidation serves as a continuous incentive for future research, which will be devoted to fuel formation at different oxidation stages, and fuel combustion, which is the main reaction determining the stability of the combustion front.

AUTHOR INFORMATION

Corresponding Authors

Mohammed A. Khelkhal – Institute of Geology and Petroleum Technologies, Kazan Federal University, Kazan 420008, Russia; orcid.org/0000-0001-7922-4004; Email: amine.khelkhal@gmail.com

Alexey V. Vakhin – Institute of Geology and Petroleum Technologies, Kazan Federal University, Kazan 420008, Russia; orcid.org/0000-0002-5168-7063; Email: Vahina_v@mail.ru

Authors

Alexandra S. Ushakova – A.N. Nesmeyanov Institute of Organoelement Compounds RAS, Moscow 119991, Russia; LLC «Gazpromneft—Technological Partnership», St. Petersburg 190000, Russia; orcid.org/0000-0002-6717-7316

Vladislav Zatsëpin – LLC «Argentum- Energy» Podolsk, Moscow 142116, Russia

Sergey A. Sitnov – Institute of Geology and Petroleum Technologies, Kazan Federal University, Kazan 420008, Russia

Complete contact information is available at:

<https://pubs.acs.org/10.1021/acs.energyfuels.2c00965>

Notes

The authors declare no competing financial interest.

ACKNOWLEDGMENTS

This work was supported by the Ministry of Science and Higher Education of the Russian Federation under agreement No. 075-15-2020-931 within the framework of the development program for a world-class Research Center “Efficient development of the global liquid hydrocarbon reserves”.

REFERENCES

- (1) Panait-Patică, A.; Serban, D.; Ilie, N.; Pavel, L.; Barsan, N. Suplacu de Barcău Field - a Case History of a Successful In-Situ Combustion Exploitation. In *SPE Europec/EAGE Annual Conference and Exhibition*; Society of Petroleum Engineers: Vienna, 2006; p 10.
- (2) Gutierrez, D.; Miller, R. J.; Taylor, A. R.; Thies, P.; Kumar, V. Buffalo Field High-Pressure Air Injection Projects 1977 to 2007: Technical Performance and Operational Challenges. *SPE Reservoir Eval. Eng.* **2009**, *12*, 542–550.
- (3) Turta, A. T.; Chattopadhyay, S. K.; Bhattacharya, R. N.; Condrachi, A.; Hanson, W. Current Status of Commercial In Situ Combustion Projects Worldwide. *J. Can. Pet. Technol.* **2007**, *46*, No. 11.
- (4) Khelkhal, M. A.; Eskin, A. A.; Nurgaliev, D. K.; Vakhin, A. V. Thermal Study on Stabilizing Combustion Front via Bimetallic Mn@Cu Talates during Heavy Oil Oxidation. *Energy Fuels* **2019**, *34*, 5121–5127.
- (5) Farhadian, A.; Khelkhal, M. A.; Tajik, A.; Lapuk, S. E.; Rezaeisadat, M.; Eskin, A. A.; Rodionov, N. O.; Vakhin, A. V. Effect of Ligand Structure on the Kinetics of Heavy Oil Oxidation: Toward Biobased Oil-Soluble Catalytic Systems for Enhanced Oil Recovery. *Ind. Eng. Chem. Res.* **2021**, *60*, 14713–14727.
- (6) Sarathi, P. S. *In-Situ Combustion Handbook—Principles and Practices*. National Petroleum Technology Office: Tulsa, OK (US); 1999 DOI: 10.2172/3175.
- (7) Mahdavi, E.; Zebarjad, F. S. *Screening Criteria of Enhanced Oil Recovery Methods Fundamentals of Enhanced Oil and Gas Recovery from Conventional and Unconventional Reservoirs*; Elsevier: Amsterdam, 2018.
- (8) Zhu, Z.; Liu, C.; Chen, Y.; Gong, Y.; Song, Y.; Tang, J. In-Situ Combustion Simulation from Laboratory to Field Scale. *Geofluids* **2021**, *2021*, 1–12.
- (9) Kovscek, A. R.; Castanier, L. M.; Gerritsen, M. G. Improved Predictability of In-Situ-Combustion Enhanced Oil Recovery. *SPE Reservoir Eval. Eng.* **2013**, *16*, 172–182.
- (10) Chattopadhyay, S. K.; Binay, R.; Bhattacharya, R. N.; Das, T. K. Enhanced Oil Recovery by In-Situ Combustion Process in Santhal Field of Cambay Basin, Mehsana, Gujarat, India—A Case Study. In *SPE/DOE Symposium on Improved Oil Recovery*; OnePetro, 2004.
- (11) Gutierrez, D.; Moore, R. G.; Mehta, S. A.; Ursenbach, M. G.; Skoreyko, F. The Challenge of Predicting Field Performance of Air Injection Projects Based on Laboratory and Numerical Modeling. *J. Can. Pet. Technol.* **2009**, *48*, 23–24.
- (12) Burger, J. G. Chemical Aspects of In-Situ Combustion - Heat of Combustion and Kinetics. *Soc. Pet. Eng. J.* **1972**, *12*, 410–422.
- (13) Millour, J. P.; Moore, R. G.; Bennion, D. W.; Ursenbach, M. G.; Gie, D. N. An Expanded Compositional Model for Lowtemperature Oxidation of Athabasca Bitumen. *J. Can. Pet. Technol.* **1987**, *26*, No. 03.
- (14) Yuan, C.; Emelianov, D. A.; Varfolomeev, M. A.; Pu, W.; Ushakova, A. S. Oxidation Behavior and Kinetics of Eight C₂₀–C₅₄ n-Alkanes by High Pressure Differential Scanning Calorimetry (HP-DSC). *Energy Fuels* **2018**, *32*, 7933–7942.
- (15) Ushakova, A.; Emelianov, D.; Zatsëpin, V.; Varfolomeev, M. In *The Free Radical Chain Mechanism of the Initial Stages of Crude Oil Oxidation in Term of SARA Fractions*, IOP Conference Series: Earth and Environmental Science; IOP Publishing, 2018; Vol. 155, p 12013.
- (16) Pu, W.-F.; Ushakova, A.; Zatsëpin, V. Chain Reactions Approach to the Initial Stages of Crude Oil Oxidation. *Energy Fuels* **2018**, *32*, 11936–11946.
- (17) Freitag, N. P. Chemical-Reaction Mechanisms That Govern Oxidation Rates during in-Situ Combustion and High-Pressure Air Injection. *SPE Reservoir Eval. Eng.* **2016**, *19*, 645–654.
- (18) Kristensen, M. R.; Gerritsen, M. G.; Thomsen, P. G.; Michelsen, M. L.; Stenby, E. H. An Equation-of-State Compositional in-Situ Combustion Model: A Study of Phase Behavior Sensitivity. *Transp. Porous Media* **2009**, *76*, 219–246.
- (19) Ushakova, A.; Zatsëpin, V.; Varfolomeev, M.; Emelianov, D. Study of the Radical Chain Mechanism of Hydrocarbon Oxidation for in Situ Combustion. *J. Combust.* **2017**, *2017*, No. 2526596.
- (20) Sequera, B.; Moore, R. G.; Mehta, S. A.; Ursenbach, M. G. Numerical Simulation of In-Situ Combustion Experiments Operated under Low Temperature Conditions. *J. Can. Pet. Technol.* **2010**, *49*, 55–64.
- (21) Lapene, A.; Debenest, G.; Quintard, M.; Castanier, L. M.; Gerritsen, M. G.; Kovscek, A. R. Kinetics Oxidation of Heavy Oil. 2. Application of Genetic Algorithm for Evaluation of Kinetic Parameters. *Energy Fuels* **2015**, *29*, 1119–1129.
- (22) Varfolomeev, M. A.; Nagrimanov, R. N.; Galukhin, A. V.; Vakhin, A. V.; Solomonov, B. N.; Nurgaliev, D. K.; Kok, M. V. Contribution of Thermal Analysis and Kinetics of Siberian and Tatarstan Regions Crude Oils for in Situ Combustion Process. *J. Therm. Anal. Calorim.* **2015**, *122*, 1375–1384.
- (23) Vargas, J. A. V.; dos Santos, R. G.; Trevisan, O. V. Evaluation of Crude Oil Oxidation by Accelerating Rate Calorimetry. *J. Therm. Anal. Calorim.* **2013**, *113*, 897–908.
- (24) Li, P.; Liu, Z.; Feng, C.; Zhao, Y.; Li, M.; Wang, X. Experimental Study on the Safety of Exhaust Gas in the Air Injection Process for Light Oil Reservoirs. *Energy Fuels* **2016**, *30*, 4504–4508.
- (25) Pu, W.-F.; Yuan, C.-D.; Jin, F.-Y.; Wang, L.; Qian, Z.; Li, Y.-B.; Li, D.; Chen, Y.-F. Low-Temperature Oxidation and Characterization

- of Heavy Oil via Thermal Analysis. *Energy Fuels* **2015**, *29*, 1151–1159.
- (26) Bhattacharya, S.; Mallory, D. G.; Moore, R. G.; Ursenbach, M. G.; Mehta, S. A. Vapor-Phase Combustion in Accelerating Rate Calorimetry for Air-Injection Enhanced-Oil-Recovery Processes. *SPE Reservoir Eval. Eng.* **2017**, *20*, 669–680.
- (27) Li, J.; Mehta, S. A.; Moore, R. G.; Zalewski, E.; Ursenbach, M. G.; Van Fraassen, K. G. In *Investigation of the Oxidation Behaviour of Hydrocarbon and Crude Oil Samples Utilizing DSC Thermal Techniques*, Canadian International Petroleum Conference; OnePetro, 2004.
- (28) Niu, B.; Ren, S.; Liu, Y.; Wang, D.; Tang, L.; Chen, B. Low-Temperature Oxidation of Oil Components in an Air Injection Process for Improved Oil Recovery. *Energy Fuels* **2011**, *25*, 4299–4304.
- (29) Sarma, H. K.; Yazawa, N.; Moore, R. G.; Metha, S. A.; Okazawa, N. E.; Ferguson, H.; Ursenbach, M. G. Screening of Three Light-Oil Reservoirs for Application of Air Injection Process by Accelerating Rate Calorimetric and TG/PDSC Tests. *J. Can. Pet. Technol.* **2002**, *41*, No. 03.
- (30) Lu, T.; Ban, X.; Guo, E.; Li, Q.; Gu, Z.; Peng, D. Cyclic In-Situ Combustion Process for Improved Heavy Oil Recovery after Cyclic Steam Stimulation. *SPE J.* **2022**, *27*, 1447–1461.
- (31) Wang, L.; Wang, J.; Pu, W.; Wang, T. Combustion Behavior and Kinetics Analysis of Isothermal Oxidized Oils from Fengcheng Extra-Heavy Oil. *Energies* **2021**, *14*, No. 6294.
- (32) Kök, M. V.; Sztatisz, J.; Pokol, G. High-Pressure DSC Applications on Crude Oil Combustion. *Energy Fuels* **1997**, *11*, 1137–1142.
- (33) Varfolomeev, M. A.; Nurgaliev, D. K.; Kok, M. V. Calorimetric Study Approach for Crude Oil Combustion in the Presence of Clay as Catalyst. *Pet. Sci. Technol.* **2016**, *34*, 1624–1630.
- (34) Kök, M. V.; Varfolomeev, M. A.; Nurgaliev, D. K. Thermal Characterization of Crude Oils by Pressurized Differential Scanning Calorimeter (PDSC). *J. Pet. Sci. Eng.* **2019**, *177*, 540–543.
- (35) Anderson, T. I.; Kovscek, A. R. Analysis and Comparison of In-Situ Combustion Chemical Reaction Models. *Fuel* **2022**, *311*, No. 122599.
- (36) Klippenstein, S. J.; Cavallotti, C. Ab Initio Kinetics for Pyrolysis and Combustion Systems. In *Computer Aided Chemical Engineering*; Elsevier, 2019; Vol. 45, pp 115–167.
- (37) Denisov, E. T.; Afanas'ev, I. B. *Oxidation and Antioxidants in Organic Chemistry and Biology*, CRC press, 2005.
- (38) Westbrook, C. K.; Pitz, W. J.; Herbinet, O.; Curran, H. J.; Silke, E. J. A Comprehensive Detailed Chemical Kinetic Reaction Mechanism for Combustion of N-Alkane Hydrocarbons from n-Octane to n-Hexadecane. *Combust. Flame* **2009**, *156*, 181–199.
- (39) Wang, T.; Wang, J.; Yang, W.; Yang, D. Quantification of Low-temperature Oxidation of Light Oil and Its SAR Fractions with TG-DSC and TG-FTIR Analysis. *Energy Sci. Eng.* **2020**, *8*, 376–391.
- (40) Jiang, X.; Yang, S.; Zhou, B.; Song, W.; Cai, J.; Xu, Q.; Zhou, Q.; Yang, K. The Variations of Free Radical and Index Gas CO in Spontaneous Combustion of Coal Gangue under Different Oxygen Concentrations. *Fire Mater.* **2022**, *46*, 549–559.
- (41) Emanuel, N. M. In *Present State of the Theory of Chain Reactions in the Liquid Phase Oxidation of Hydrocarbons*, 7th World Petroleum Congress; OnePetro, 1967.
- (42) Freitag, N. P.; Verkoczy, B. In *Low-Temperature Oxidation of Oils in Terms of Sara Fractions: Why Simple Reaction Models Don't Work*, Canadian International Petroleum Conference; Petroleum Society of Canada: Calgary, 2003; p 17.
- (43) Freitag, N. P. Evidence That Naturally Occurring Inhibitors Affect the Low-Temperature Oxidation Kinetics of Heavy Oil. *J. Can. Pet. Technol.* **2010**, *49*, 36–41.
- (44) Mehrabi-Kalajahi, S. S.; Varfolomeev, M. A.; Yuan, C.; Emelianov, D. A.; Khayarov, K. R.; Klimovitskii, A. I.; Rodionov, A. A.; Orlinkii, S. B.; Gafurov, M. R.; Afanasiev, I. S.; et al. EPR as a Complementary Tool for the Analysis of Low-Temperature Oxidation Reactions of Crude Oils. *J. Pet. Sci. Eng.* **2018**, *169*, 673–682.

- (45) Klinchev, V. A.; Zatsepin, V. V.; Ushakova, A. S.; Telyshev, S. V. In *Laboratory Studies and Implementation of In-Situ Combustion Initiation Technology for Air Injection Process in the Oil Reservoirs*, SPE Russian Oil and Gas Exploration & Production Technical Conference and Exhibition; OnePetro, 2014.

Recommended by ACS

Detailed Microkinetics for the Oxidation of Exhaust Gas Emissions through Automated Mechanism Generation

Bjarne Kreitz, Olaf Deutschmann, *et al.*

AUGUST 30, 2022
ACS CATALYSIS

READ 

Comparison and Analysis of Butanol Combustion Mechanisms

Martin Bolla, Tamás Turányi, *et al.*

SEPTEMBER 01, 2022
ENERGY & FUELS

READ 

Experimental and Kinetic Studies of Ethylene Glycol Autoignition at High Temperatures

Ping Xu, Changhua Zhang, *et al.*

MARCH 04, 2022
ACS OMEGA

READ 

Formation and Combustion Heat Release of Naphthenic-Based Crude Oil Cokes at Different Reaction Temperatures

Rigu Su, Yong Guo, *et al.*

APRIL 19, 2022
ACS OMEGA

READ 

Get More Suggestions >